Modeling and Simulation of the Sequencing Batch Reactor at a Full-Scale Municipal Wastewater Treatment Plant

Bing-Jie Ni, Wen-Ming Xie, Shao-Gen Liu, and Han-Qing Yu
Dept. of Chemistry, University of Science & Technology of China, Hefei 230026 China

Ying-Zhe Wang, Gan-Wang, and Xian-Liang Dai
Anhui Guozhen Environmental Engineering Co., Hefei 230088 China

DOI 10.1002/aic.11820
Published online June 23, 2009 in Wiley InterScience (www.interscience.wiley.com).

In this work, we attempted to modify the Activated Sludge Model No.3 and to simulate the performance of a full-scale sequencing batch reactor (SBR) plant for municipal wastewater treatment. The long-term dynamic data from the continuous operation of this SBR plant were simulated. The influent wastewater composition was characterized using batch measurements. After incorporating all the relevant processes, the sensitivity of the stoichiometric and kinetic coefficients for the model was thoroughly analyzed prior to the model calibration. The modified model was calibrated and validated with the data from both batch- and full-scale experiments. Model predictions were compared with routine data in terms of chemical oxygen demand, NH_4^+-N and mixed liquid volatile suspended solids in the SBR, combined with batch experimental data under different conditions. The model predictions match the experimental results well, demonstrating that the model is appropriate to simulate the performance of a full-scale wastewater treatment plant even operated under perturbation conditions.
 AIChE J, 55: 2186–2196, 2009
Keywords: activated sludge, calibration, characterization, model, sequencing batch reactor (SBR), simulation, validation, wastewater treatment plant (WWTP)

Introduction

The sequencing batch reactor (SBR) has been widely used to treat municipal wastewater,[1–4] landfill leachates,[5] and various industrial wastewaters since it was invented by Irvine and his coworkers.[1,6–8] The SBR is a fill-and-draw system, where each tank is subjected to the following operations: fill (static or mixed), react (static or mixed), settle, idle, and decant (or draw) for predetermined time periods. These periods can be used for various microbial reactions requiring different environmental conditions.[8] The major advantage of the SBR is that the periods can be rearranged, or even omitted, depending on design goals. In addition, the system does not require much space and separate clarifiers, because all the activated sludge processes are conducted within time in one tank rather than in separate tanks. Also, the duration of each cycle can be varied according to the influent dynamics. The operating costs associated with aeration energy could be saved if the aeration cycle can be terminated after the desirable reactions were completed. All of these advantages of an SBR system make it a favorable option for both municipal and industrial wastewater treatment, especially in developing countries like China.

Mathematical modeling has been proven to be essential for understanding complex microbial systems, such as activated sludge processes in a SBR system.[9] It is an inherent

Correspondence concerning this article should be addressed to H.-Q. Yu at hqyu@ustc.edu.cn

Table 1. Equations for All Components in the Established Model

Component	Nonsteady-State Mass Balance Equation	No.
Mass balance for X_S	$\frac{dX_S}{dt} = -k_H \frac{X_S/X_H}{K_X + X_S/X_H} X_H$	(1)
Mass balance for S_S	$\frac{dS_S}{dt} = -\frac{dX_S}{dt} - \frac{1}{Y_{STO}} q_1 - \frac{1}{Y_{STO}} q_2 - \frac{1}{Y_{H,S}} q_3 - \frac{1}{Y_{H,S}} q_4$	(2)
Mass balance for S_{NH_4}	$\frac{dS_{NH_4}}{dt} = -i_{NSI} \frac{dX_S}{dt} - i_{NBM} q_3 - i_{NBM} q_4 - i_{NBM} q_5 - i_{NBM} q_6 - (i_{NBM} + 1/Y_A) q_{11} + (i_{NBM} - f_I i_{NXI})(q_7 + q_8 + q_{12} + q_{13})$	(3)
Mass balance for S_{NO_3}	$\frac{dS_{NO_3}}{dt} = -\frac{1 - Y_{STO}}{2.86 Y_{STO}} q_2 - \frac{1 - Y_{H,S}}{2.86 Y_{H,S}} q_4 - \frac{1 - Y_{H,STO}}{2.86 Y_{H,STO}} q_6 - \frac{1 - f_I}{2.86} q_8 - \frac{1}{2.86} q_{10} + \frac{1}{Y_A} q_{11} - \frac{1 - f_I}{2.86} q_{13}$	(4)
Mass balance for S_{N_2}	$\frac{dS_{N_2}}{dt} = -\frac{dS_{NO_3}}{dt} + \frac{1}{Y_A} q_{11}$	(5)
Mass balance for X_{STO}	$\frac{dX_{STO}}{dt} = q_1 + q_2 - \frac{1}{Y_{H,STO}} q_5 - \frac{1}{Y_{H,STO}} q_6 - q_9 - q_{10}$	(6)
Mass balance for X_H	$\frac{dX_H}{dt} = q_3 + q_4 + q_5 + q_6 - q_7 - q_8$	(7)
Mass balance for X_A	$\frac{dX_A}{dt} = q_{11} - q_{12} - q_{13}$	(8)
Mass balance for X_I	$\frac{dX_I}{dt} = f_I q_7 + f_I q_8 + f_I q_{12} + f_I q_{13}$	(9)
Mass balance for S_O	$\frac{dS_O}{dt} = -\frac{1 - Y_{STO}}{Y_{STO}} q_1 - \frac{1 - Y_{H,S}}{Y_{H,S}} q_3 - \frac{1 - Y_{H,STO}}{Y_{H,STO}} q_5 - (1 - f_I) q_7 - q_9 - \frac{4.57 - Y_A}{Y_A} q_{11} - (1 - f_I) q_{12}$	(10)

element of the engineering practice dealing with the optimal design and operation of wastewater treatment plants (WWTPs). Dynamic simulation of the processes in a WWTP is a useful tool in the selection of operational strategies that improve process stability, effluent quality, and save operational costs. Optimum solutions for the design and operation of a WWTP include the mutual relationships among the different process elements involved in wastewater and activated sludge. Therefore, when models are developed to simulate a WWTP, a dynamic description of all the relevant processes in the activated sludge system should be taken into account.

The Activated Sludge Models (ASMs) introduced by the International Water Association (IWA) such as Activated Sludge Model No.1 (ASM1) and Activated Sludge Model No.3 (ASM3),[10] focus on the heterogeneity of substrate and biomass types and are suitable for simulation of a full-scale WWTP. The ASM1 was developed primarily for municipal treatment plants to simulate the removal of organic carbon and ammonium-N,[11] whereas the subsequent ASM3 was established to overcome a number of problems that have emerged from the applications of ASM1.[10,12] In ASM3, the storage of organic substrates is included as a new process, and lysis is replaced by an endogenous respiration process. As a result, the hydrolysis becomes less important for the rates of oxygen consumption and denitrification and is now independent of the electron donor, compared with the ASM1. Furthermore, the rates of all processes (except for hydrolysis) under anoxic conditions are lower than those under aerobic conditions. In ASM3, smaller anoxic yield coefficients are used.[12] ASM1 has been used over a decade for modeling the removal of organic matter and nitrification and denitrification processes. As a result, considerable experience has been acquired with this model. However, it is a different case for ASM3, because it has not been applied to simulate full-scale WWTPs yet.

Therefore, the main objective of this study was to modify ASM3 and to simulate the performance of a full-scale SBR plant for municipal wastewater treatment. After incorporating all the relevant processes, the model could be validated and used as a decision tool for predicting the activated sludge process in full-scale WWTPs. An extensive literature search did not reveal any other attempts to simulate a full-scale SBR plant for municipal wastewater treatment using ASM3.

Model description

In ASM3, all readily biodegradable substrate was assumed to be initially stored as internal storage products before being used for growth. As a modification, in our work the aerobic/anoxic simultaneous storage and growth on organic substrates are assumed. The modified model describes the relationships among the five solid species: slowly biodegradable substrate, heterotrophic microorganisms, autotrophic microorganisms, storage products of heterotrophic microorganisms, and

Table 2. Kinetics Rate Expressions for the Established Model

Heterotrophic Microorganisms	
Aerobic storage of S_S	$q_1 = k_{STO} M_S M_O X_H$
Anoxic storage of S_S	$q_2 = k_{STO} \eta_{NO_x} M_S I_O M_{NO_3} X_H$
Aerobic growth on S_S	$q_3 = \mu_{H,S} M_S M_O M_{NH_4} X_H$
Anoxic growth on S_S	$q_4 = \mu_{H,S} \eta_{NO_x} M_S I_O M_{NO_3} M_{NH_4} X_H$
Aerobic growth on X_{STO}	$q_5 = \mu_{H,STO} M_{STO} I_S M_O M_{NH_4} X_H$
Anoxic growth on X_{STO}	$q_6 = \mu_{H,STO} \eta_{NO_x} M_{STO} I_S I_O M_{NO_3} M_{NH_4} X_H$
Aerobic endogenous respiration	$q_7 = b_H M_O X_H$
Anoxic endogenous respiration	$q_8 = b_{H,NO_x} I_O M_{NO_3} X_H$
Aerobic respiration of X_{STO}	$q_9 = b_{STO} M_O X_{STO}$
Anoxic respiration of X_{STO}	$q_{10} = b_{STO,NO_x} I_O M_{NO_3} X_{STO}$
Autotrophic microorganisms	
Aerobic growth	$q_{11} = \mu_A M_{A,O} M_{A,NH_4} X_A$
Aerobic endogenous respiration	$q_{12} = b_A M_{A,O} X_A$
Anoxic endogenous respiration	$q_{13} = b_{A,NO_x} I_{A,O} M_{NO_3} X_A$

residual inert biomass; three soluble species: readily biodegradable substrate, ammonia (NH_4^+-N), and dissolved nitrogen; and two electron acceptors, which are dissolved oxygen (DO) and nitrate (NO_3^--N). The present model uses the following symbols for concentrations: slowly biodegradable substrate (X_S), heterotrophic microorganisms (X_H), autotrophic microorganisms (X_A), heterotrophic storage products (X_{STO}), residual inert biomass (X_I), readily biodegradable substrate (S_S), ammonia (S_{NH_4}), dissolved nitrogen (S_{N_2}), dissolved oxygen (S_O), and nitrate (S_{NO_3}). The units for all species are oxygen demand or oxygen (for DO), which is directly proportional to electron equivalents (8 g O_2 per e^- equivalent).

The nonsteady-state mass balances for all model components are written as Eqs. 1–10 in Table 1, whereas the corresponding process rate expressions are given in Table 2. For the heterotrophs, $M_S = \frac{S_S}{K_S + S_S}$ and $M_O = \frac{S_O}{K_O + S_O}$ are Monod kinetic functions for the external substrate and DO, respectively. $I_O = \frac{K_O}{K_O + S_O}$ is a Monod-type inhibition function for the effect of DO on anoxic biological reactions, and $M_{NO_3} = \frac{S_{NO_3}}{K_{NO_3} + S_{NO_3}}$ is Monod kinetic functions for nitrate. $M_{NH_4} = \frac{S_{NH_4}}{K_{NH_4} + S_{NH_4}}$ is Monod kinetic functions for ammonia for heterotrophic growth. $M_{STO} = \frac{X_{STO}/X_H}{K_{STO} + X_{STO}/X_H}$ stands for a saturation-kinetic function for utilization of X_{STO}, and $I_S = \frac{K_S}{K_S + S_S}$ is a Monod-type inhibition function for the effect of high S_S on utilization of X_{STO}. In this approach, X_{STO} is used to support synthesis of active heterotrophic biomass when usual synthesis is precluded by low S_S. For the autotrophs, $M_{A,NH_4} = \frac{S_{A,NH_4}}{K_{A,NH_4} + S_{A,NH_4}}$ and $M_{A,O} = \frac{S_O}{K_{A,O} + S_O}$ are Monod kinetic functions for ammonia and DO, respectively. $I_{A,O} = \frac{K_{A,O}}{K_{A,O} + S_O}$ is the Monod-type inhibition function for the effect of DO on anoxic endogenous respiration of X_A. For the mass balance equations for the influent filling period, each mass balance has an advective term, $QS^0/V - QS/V$; where V is the liquid volume, Q is the flow rate, and S^0 and S represent the influent and reactor concentrations, respectively. Rate terms in each mass balance are explained in the equations shown in Tables 1 and 2.

Table 3. Characteristics of the Influent and Effluent as well as Key Reactor Constituents for the Full-Scale SBR Plant (the standard Deviations are Listed in Parentheses After the Average Values)

Characteristics	Reactor Constituents	Influent	Effluent
SVI (mL g^{-1})	85 (20)	–	–
MLSS (mg L^{-1})	4000 (1500)	–	–
MLVSS (mg L^{-1})	2400 (1000)	–	–
COD (mg L^{-1})	–	160 (70)	40 (10)
BOD_5 (mg L^{-1})	–	60 (20)	1.5 (2)
NH_4^+-N (mg L^{-1})	–	30 (15)	4 (3.5)
NO_2^--N (mg L^{-1})	–	0.1 (0.1)	6 (4)
NO_3^--N (mg L^{-1})	–	0.5 (0.5)	17 (6)
Total N (mg L^{-1})	–	35 (20)	25 (10)
VSS (mg L^{-1})	–	90 (40)	10 (9)

Materials and Methods

Process description of the Zhuzhuanjing WWTP

The Zhuzhuanjing WWTP is located in Hefei City, China, in which wastewater originating from the surrounding city areas is treated. The plant consists of gridirons, primary clarifiers, and eight sets of SBRs. Each SBR has a rectangle configuration and is operated in a fill-and-draw mode. Wastewater is introduced and simultaneously mixed in the fill period; the reactor is aerated in the reaction period; later, the mixed liquor is allowed to settle in the settling period; at the end of each cycle, the supernatant is discharged from the reactor. The working volume of each SBR is 2000 m^3. The time allotted for each SBR operating cycle is 30 min for fill, 120 min for react, 60 min for settle, and 30 min for decant. The wastewater characteristics (including average and

Table 4. Measurements for the Characterization of Wastewater

Definition	Symbol	Unit	Average Value	Source of Data
Influent total COD	COD_{inf}	g COD m^{-3}	212.6	Measurement
Influent COD in filtered sample	$COD_{f,inf}$	g COD m^{-3}	84.6	Measurement
Influent BOD_5	BOD_5	g BOD_5 m^{-3}	91.4	Measurement
Effluent COD in filtered sample	$COD_{f,eff}$	g COD m^{-3}	27.9	Measurement
Effluent COD	COD_{eff}	g COD m^{-3}	40.3	Measurement
Biodegradable COD in influent	BCOD	g COD m^{-3}	156.1	Calculation Grady et al.[18] $BCOD = \frac{BOD_5}{f_{BOD}(1 - Y_H f_{XI})}$
BOD_5/BOD_U ratio	f_{BOD}	–	0.67	Grady et al.[18]
Heterotrophic biomass yield coefficient	Y_H	g COD g^{-1} COD	0.63	Grady et al.[18]
Nonbiodegradable fraction resulting from the biomass decay	f_{XI}	–	0.2	Grady et al.[18]

Table 5. Fractionation of Organic Matters in Wastewater

Definition	Symbol	Unit	Equation
Inert soluble organic compounds	S_I	g COD m^{-3}	$0.95 \cdot COD_{f,eff}$
Readily biodegradable organic compounds	S_S	g COD m^{-3}	$COD_{f,inf} - S_I$
Slowly biodegradable organic compounds	X_S	g COD m^{-3}	$BCOD - S_S$
Inert particulate organic compounds	X_I	g COD m^{-3}	$COD_{inf} - COD_{f,inf} - X_{H,inf} - X_S$

standard deviations), key reactor constituents [sludge volume index (SVI) and mixed liquid suspended solid (MLSS), etc.], and effluent constituents are listed in Table 3.

The Zhuzhuanjing WWTP was a conventional activated sludge process. This plant was initially designed and has been operated mainly for treating organic pollutants and NH_4^+-N. Thus, the operating strategy selected at the present time was not an ideal one for effective removal of both N and P. It is true that this plant should be upgraded for a better removal of nutrients. As a useful tool for WWTP upgrading, model simulation could be used to make the best decision with the following steps: formulation of an appropriate model; characterization of the wastewater; calibration of the model; verification of the calibration; and model simulation for optimization. The developed model should be fully calibrated and evaluated with the data from the WWTP operation, which then could be used for better understanding and further optimization of this full-scale SBR plant. In addition, a well-structured model should be able to simulate the microbial consortium data under different conditions.

Simulation

In this work, all simulation and parameter estimation were performed with a nonlinear least-squares algorithm in the AQUASIM software package.[13] This program offers a free definition of the biokinetic model, flow scheme and process control strategies, graphic support of the simulation, experimental data, and communication with spreadsheet programs.[14]

Model calibration and validation procedure

Because of the complexity of the model, extensive calibration and validation procedures were applied. First, the input wastewater and biomass were characterized. Then, simulations were initially performed with the model default values, but the model required a further calibration. The calibration procedure included the long-term dynamic simulations of the performance of both full-scale SBR and the batch tests with the municipal wastewater. The one set of model parameters obtained were then applied for model validation. The other operational data from the batch tests and the full-scale SBRs were used for model validation.

Collection of the routine data of the WWTP

The recordings of routine measurements for the full-scale reactors were used as a primary source for dynamic simulation. The measurements included chemical oxygen demanded (COD), ammonia (NH_4^+-N), nitrate (NO_3^--N), nitrite (NO_2^--N), MLSS, and mixed liquid volatile suspended solid (MLVSS) concentrations. In addition, ''on-line'' recordings of flow rate, temperature, pH, and DO concentrations in the SBRs were also collected for the simulation.

Batch experiments

The batch tests were carried out using two 2-L reactors at 20°C, which were seeded with fresh activated sludge taken from the full-scale SBRs. The batch tests include the following: (i) aerobic respirometric tests with allylthiourea (ATU) (a nitrification inhibitor); (ii) aerobic respirometric tests

Table 6. Kinetic and Stoichiometric Coefficients for the Model

Parameter	Definition	Initial Values	Calibrated Values	Unit
Stoichiometry				
Y_{STO}	Yield coefficient for X_H storage	0.81	0.78	g COD g^{-1} COD
$Y_{H,S}$	Yield coefficient for X_H growth on S_S	0.58	0.56	g COD g^{-1} COD
$Y_{H,STO}$	Yield coefficient for X_H growth on X_{STO}	0.68	0.65	g COD g^{-1} COD
Y_A	Yield coefficient for X_A growth	0.24	0.24	g COD g^{-1} COD
η_{NOx}	Anoxic reduction factor	0.60	0.60	—
f_I	Fraction of X_I in respiration	0.20	0.20	g COD g^{-1} COD
i_{NBM}	Nitrogen content of biomass	0.07	0.07	g N g^{-1} COD
i_{NXI}	Nitrogen content of X_I	0.02	0.02	g N g^{-1} COD
Kinetics				
k_{STO}	Maximum storage rate of X_H	0.21	0.25	h^{-1}
$\mu_{H,STO}$	Maximum growth rate of X_H on X_{STO}	0.083	0.17	h^{-1}
$\mu_{H,S}$	Maximum growth rate of X_H on S_S	0.083	0.11	h^{-1}
K_S	Biomass affinity constant for S_S	2.00	19.7	g COD m^{-3}
K_{STO}	Biomass affinity constant for X_{STO}	1.00	0.59	g COD g^{-1} COD
K_{O_2}	Dissolve oxygen affinity constant	0.20	0.20	g O_2 m^{-3}
b_{STO}	Respiration rate coefficient of X_{STO}	0.0083	0.013	h^{-1}
b_H	Respiration rate coefficient of X_H	0.0083	0.013	h^{-1}
μ_A	Maximum growth rate of X_A	0.042	0.052	h^{-1}
b_A	Respiration rate coefficient of X_A	0.0063	0.0063	h^{-1}
K_{A,O_2}	Oxygen affinity constant for X_A	0.50	0.50	g O_2 m^{-3}
K_{NH_4}	Biomass NH_4 affinity constant	0.01	0.01	g N m^{-3}
K_{A,NH_4}	NH_4 affinity constant for X_A	1.0	4.30	g N m^{-3}
K_{NO_3}	Biomass NO_3 affinity constant	0.50	0.50	g N m^{-3}

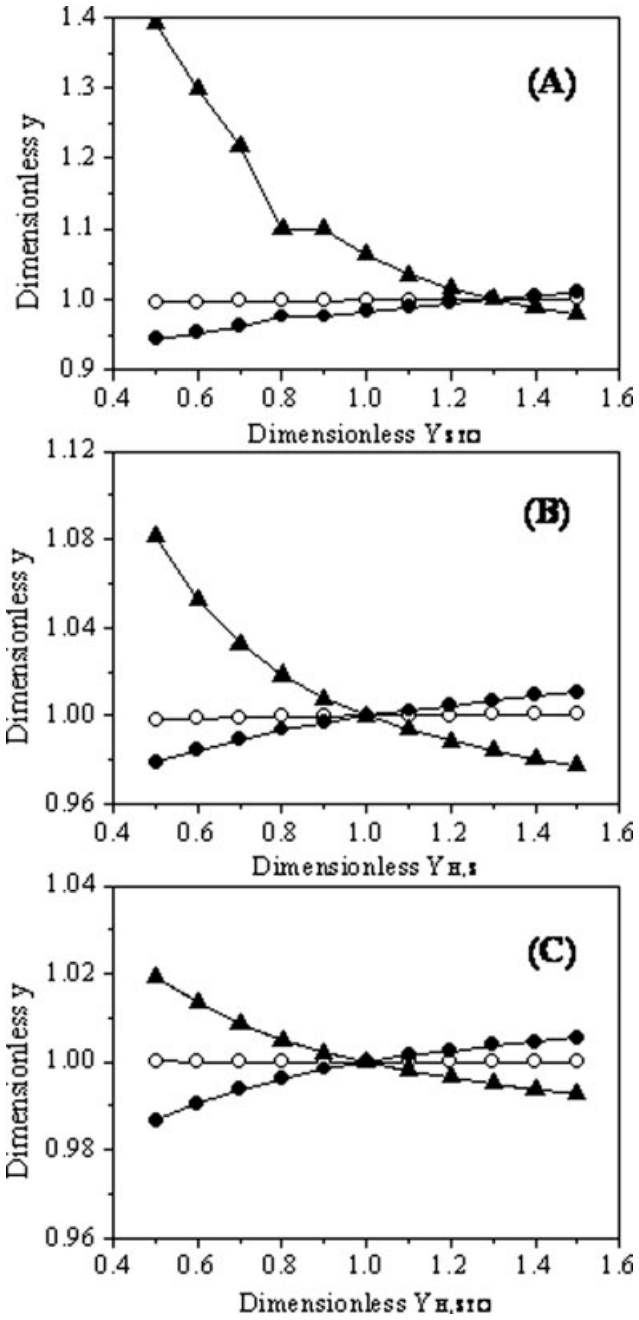

Figure 1. Effect of the stoichiometric parameters on the model outputs („ y = MLVSS; −, y = COD; 7, y = NH_4^+-N): (A) Y_{STO}; (B)$Y_{H,S}$; and (C) $Y_{H,STO}$.

without ATU; (iii) anoxic respirometric tests; and (iv) aerobic endogenous respiration tests.

Three types of initial operating conditions were applied to the batch tests: the first one with a high initial substrate/biomass (S_O/X_O) ratio (significant microbial growth), the second one with a moderate initial S_O/X_O ratio (moderate microbial growth), and the third one with a low initial S_O/X_O ratio (negligible microbial growth). For the tests with an inhibition on nitrification, 20 mg/L of ATU was added into the reactors. In the anoxic tests, nitrate was externally added at a predetermined concentration.

To obtain a high initial S_O/X_O ratio, no activated sludge was added to the reactors, in which wastewater was placed and respiration rate was measured for 1 day. In this case, only the microorganisms present in the municipal wastewater contributed to the respiration. Initial and final samples were drawn and total COD was measured. For the moderate S_O/X_O test (around 1–2 g COD/g VSS), wastewater sample with a predetermined volume was added into the reactor with aerated sludge. For the test at a low S_O/X_O ratio, a small volume of wastewater sample was added into the reactor with aerated sludge, with a ratio sufficiently low for an insignificant microbial growth but a constant endogenous respiration. This ratio has been reported to be around 0.2 g COD/g VSS.[15,16]

The batch reactors were inoculated with the activated sludge withdrawn from the full-scale SBRs at the end of the react phase, and the aeration lasted for 10 h to ensure the depletion of the external substrate. The final volume in the batch reactors was adjusted to 2 L using tap water and the endogenous respiration rate was measured for 2–3 h until it became constant. Then, a known amount of wastewater was added to the reactors to reach an S_O/X_O ratio in a range 0.01 to 2 g COD/g VSS. Samples were withdrawn from the reactors every 5–10 min, and were immediately centrifuged and then stored at 4°C for analysis.

Wastewater and biomass characterization

The organic matters in the municipal wastewater were fractionized using the results in Table 4 according to the procedures given in Table 5. The biodegradable COD (BCOD) in the influent is the sum of the readily biodegradable soluble COD (S_S) and the slowly biodegradable particulate COD (X_S).[17] The biodegradable COD (BCOD and $S_S + X_S$) concentration was calculated from the formula proposed by Grady et al.[18] The inert fraction S_I was determined independently and subtracted from the soluble COD to give the fraction S_S. S_I is evaluated from the inert COD in the effluent of the examined treatment plant. The concentrations of X_S and X_I were estimated based on the BOD_5 measurements.[19] With the presented methodology for the characterization of the organic fractions S_I, S_S, and X_S, the fraction X_I is found to be the difference between the total COD and the other fractions. The fractionation was performed on each consecutive day during the long-term simulation period.

Municipal wastewater contains a significant concentration of heterotrophs.[20] However, the concentration of heterotrophs in the municipal wastewater is not important relative to the biomass enriched for and maintained in the reactor and should not be taken into account. In the ASMs, the concentration of the heterotrophic biomass in wastewater, X_H, is assumed to be negligible.[17] Therefore, in this work, the concentration of heterotrophs in the municipal wastewater was not taken into account.

Analytical methods

The DO concentration was measured with a DO electrode (MO128, Mettler-Toledo, Switzerland). Sludge morphology was observed using an optical microscope (Olympus

CX41). Measurements of COD, NH_4^+-N, NO_3^--N, NO_2^-N, MLSS, and MLVSS followed the Standard Methods.[21] The oxygen uptake rate (OUR) was determined from the measurement of the DO profiles in an air-tight vessel, as described previously.[22]

Results and Discussion

Wastewater characterization

The average contribution of the individual model components to the total influent COD in the period of January 2007–May 2007 is calculated according to Tables 4 and 5. During the simulation period, the influent COD fraction did not change substantially from the average values with a maximum difference less than 1.4%. The estimated S_S fraction is determined to be 30.1% ± 3.9% of the total COD, and this value is comparable with the results of other studies,[19,23,24] in which the S_S concentration of the settled wastewater constitutes 26–32% of the total COD. The initially S_I fraction is estimated to be 10.3% ± 2.3% of the total COD. The initially established X_I fraction, approximately 11% of the total COD, lies within the range of 10–29% reported in the literature.[19,23–26] The contribution of X_S is calculated to be 43.6% of the total COD. Thus, the $S_S/(S_S+X_S)$ ratio is calculated and the values remain within the suggested range of 0.3–0.5.[24]

Sensitivity analysis

Prior to the model calibration, sensitivity analysis should be conducted to evaluate the most important parameters in the model, which should be strictly kept under control in the

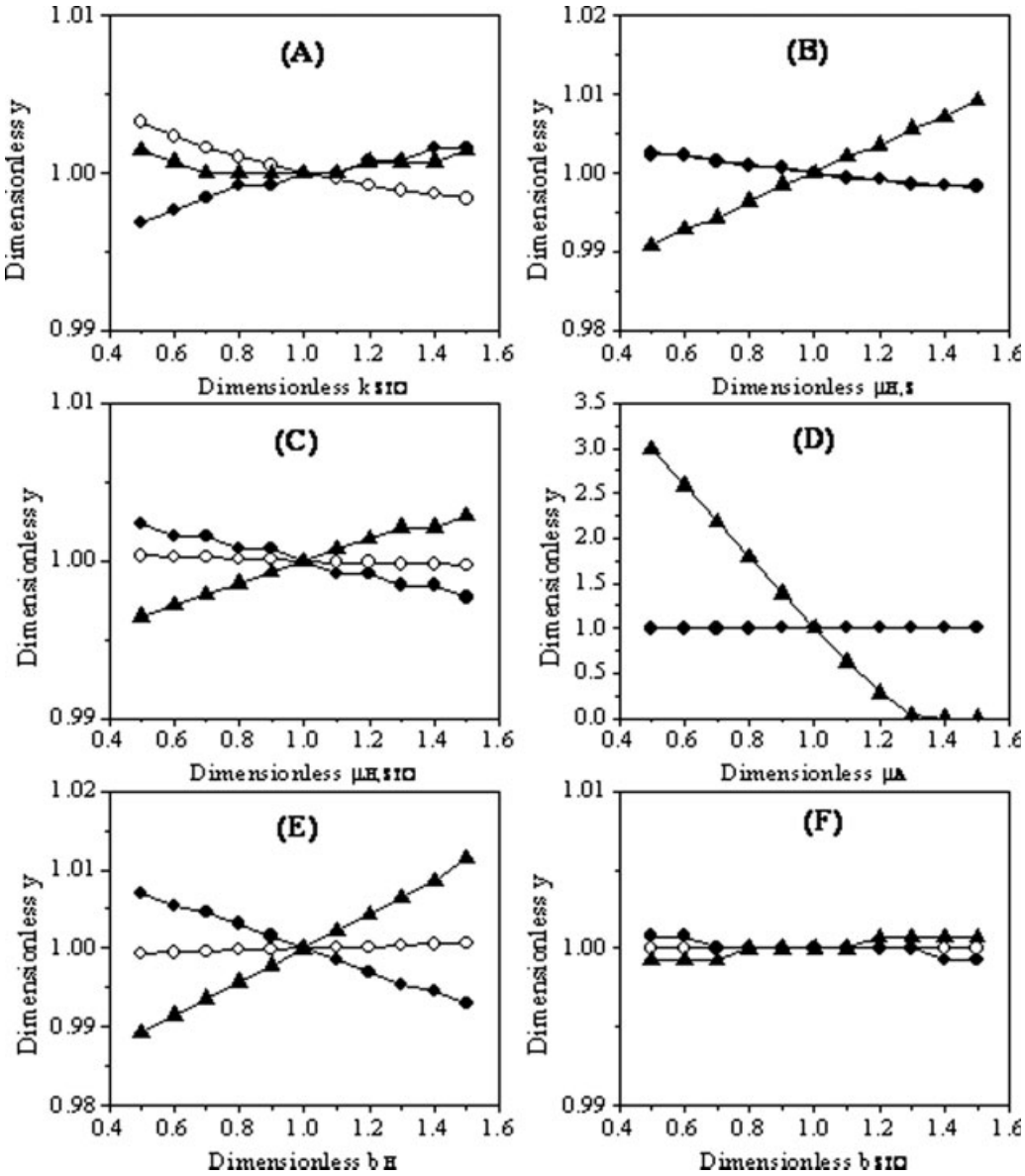

Figure 2. Effect of the kinetic parameters on the model outputs (,, y = MLVSS; −, y = COD; 7, y = NH_4^+-N): (A) k_{STO}; (B) $\mu_{H,S}$; (C) $\mu_{H,STO}$; (D) μ_A; (E) b_H; and (F) b_{STO}.

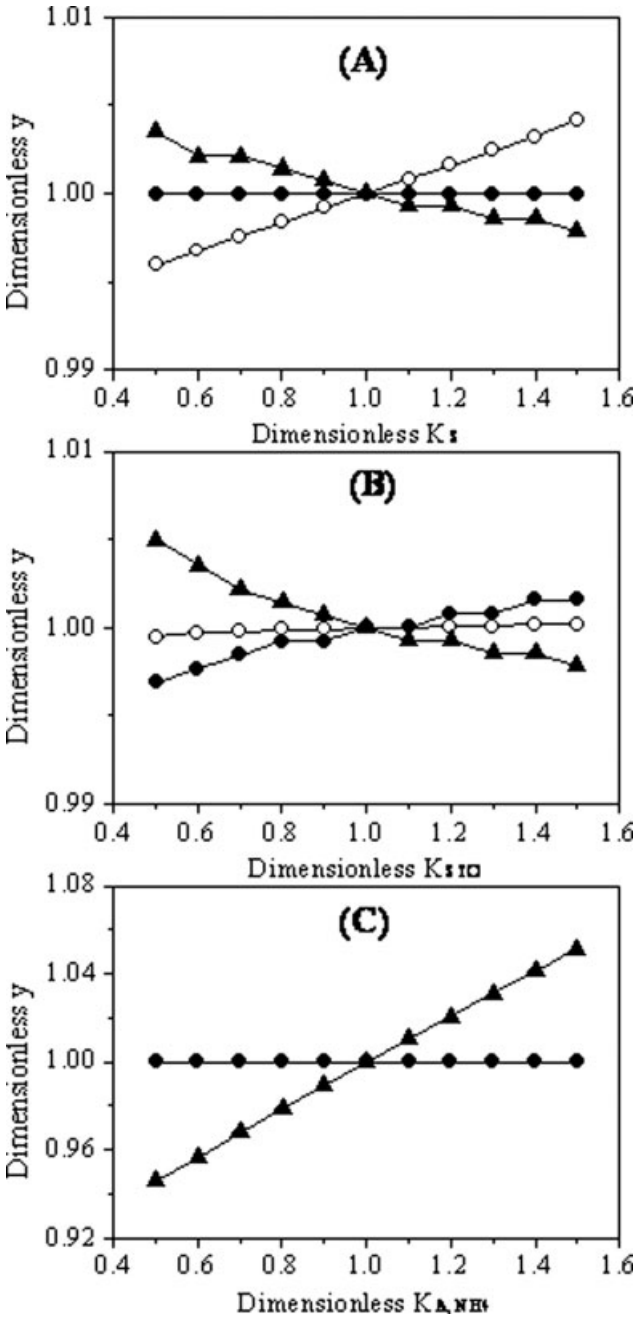

Figure 3. Effect of the values of affinity constant parameters on the model outputs („ y = MLVSS; −, y = COD; 7, y = NH_4^+-N): (A) K_S; (B) K_{STO}; and (C) K_{A,NH_4}.

calibration and model validation.[27,28] In the sensitivity analysis, the behavior of the model is evaluated as a consequence of a variation of the input parameters and is performed using a one-variable-at-a-time approach. The sensitivity coefficient represents the change in the output variable, resulting from a change in the input variable. The sensitivity analysis is conducted using the curve profiles of output with input variables. Dimensionless values are used by dividing the basic variables for input ones or the corresponding output results. The model parameters are independent, and they are investigated individually. All model coefficients, including kinetic and stoichiometric coefficients, are changed one by one in the simulation. Parameters are assigned with initial values for calibration from literatures as shown in Table 6.[10,29] In this work, the most important model output variables of COD, NH_4^+-N and MLVSS concentrations are analyzed as shown in Figures 2–4.

Effect of Stoichiometric Parameters. Heterotrophic storage of the readily biodegradable substrates plays an important role in the substrate removal. Meanwhile, the heterotrophic growth on the external substrate and the storage polymers has a considerable influence on biomass growth. In our model, three distinctive yield coefficients independent from each other stand for storage (Y_{STO}) (Figure 1A), direct growth on external substrate ($Y_{H,S}$) (Figure 1B) and growth on the internal storage products ($Y_{H,STO}$) (Figure 1C). All of them have a significant influence on the output variables, as shown in Figure 1.

It is found that ±50% fluctuation in the yield coefficient for storage will result in a maximum of 50% fluctuation in the NH_4^+-N concentration, ±10% fluctuation in the MLVSS level, and ±1% fluctuation in the effluent COD concentration. The yield coefficients for growth on the external substrate and growth on the internal storage products have similar effects on the model outputs. An increase in the three yield coefficients leads to a decrease in the effluent NH_4^+-N concentration and an increase in MLVSS level (Figure 1). This is associated with the indirect effect of the yields on the heterotrophic growth rate through influencing the concentrations of the readily biodegradable substrate and the storage polymers. The effluent COD concentration does not change substantially, mainly because of its low concentrations in the bulk liquid.

The other stoichiometric parameters, such as anoxic reduction factor (η_{NO_X}), fraction of X_I in respiration (f_I), and yield coefficient for X_A growth (Y_A), affect the model outputs to a minor extent. The concentrations of COD, NH_4^+-N, and MLVSS are practically insensitive to the changes in these parameters.

Effect of Kinetic Rate Parameters. The results of sensitivity analysis of the kinetic rate parameters are shown in Figure 2. It should be noted that, except the respiration rate coefficient of X_A (b_A), the kinetic rate parameters, especially $\mu_{H,S}$, b_H, and μ_A, significantly affect at least one of the considered model outputs.

The maximum storage rate of biomass (k_{STO}) has an influence on the model outputs (Figure 2A). The effluent NH_4^+-N concentration changes slightly with a change of the maximum anoxic storage rate. The MLVSS concentration increases, whereas COD decreases with an increase in the maximum storage rate. The maximum growth rates on substrate ($\mu_{H,S}$) and X_{STO} ($\mu_{H,STO}$) have the same sensitivities to the calculation results (Figures 2B and 2C). An increase in $\mu_{H,S}$ and $\mu_{H,STO}$ leads to a decrease in the effluent COD concentration and an increase in the effluent NH_4^+-N level. A 50% increase in the maximum growth rate of X_A (μ_A) causes a considerable decrease in the effluent NH_4^+-N concentration (Figure 2D). The endogenous decay coefficient of the heterotrophs (b_H) considerably affects both NH_4^+-N and MLVSS concentration

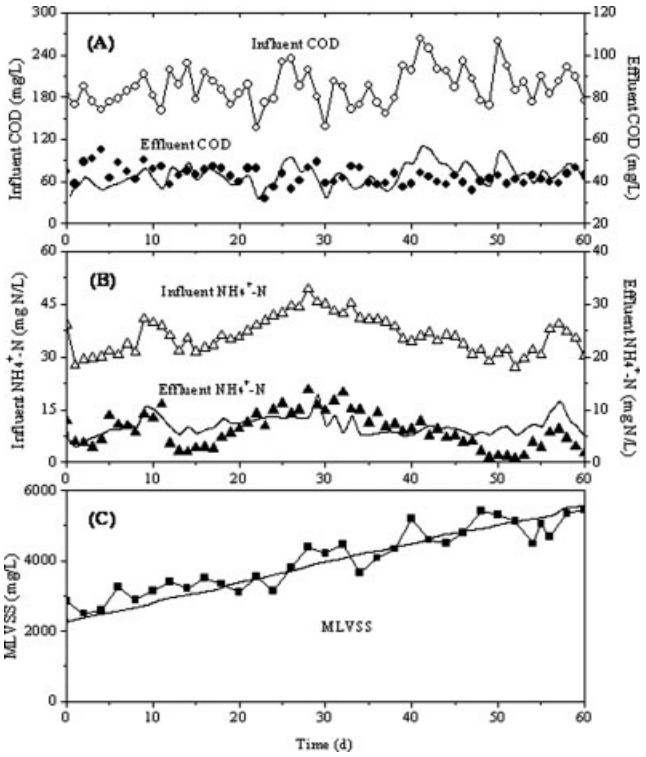

Figure 4. Measured and predicted results of the WWTP (March 4, 2007–January 2, 2007).

(A) COD level; (B) NH_4^+-N level; and (C) MLVSS concentration.

(Figure 2E). By contrast, the respiration rate coefficient of X_{STO} is not sensitive (Figure 2F).

Effect of Key Affinity Constant. Sensitivity of the key affinity constants to the model outputs is evaluated. K_S and K_{STO} are proven to be influential to the model outputs with 50% variation to the initial values (Figure 3A). With an increase in K_S, the effluent COD concentration increases, but the NH_4^+-N concentration decreases. The K_{STO} has a similar effect on the NH_4^+-N concentration, whereas the MLVSS concentration increases with the increasing K_{STO} (Figure 3B). The storage and growth on the storage polymers lead to a slower substrate consumption and biomass growth. For the NH_4^+-N affinity constant of X_A (K_{A,NH_4}), the effluent NH_4^+-N concentration substantially increases with the increasing K_{A,NH_4} (Figure 3C). However, K_{A,NH_4} has no influence on the concentrations of COD and MLVSS. The other affinity constant parameters listed in Table 6 are proven to have no substantial influence on the output COD, NH_4^+-N, and MLVSS concentrations.

The sensitivity analysis reveals that the model parameters involved in the storage process, the heterotrophic endogenous decay, and growth have a great influence on the model outputs. This provides useful information for the subsequent model calibration.

Model calibration

Model calibration procedure is a process of adjusting coefficient values of the model, so that the results produced by the model with these coefficients closely match the measured data. Our models for simulation tasks incorporate a number of stoichiometric and kinetic parameters relating to both X_H and X_A. The initial parameter values are obtained with the data in the literature as shown in Table 6. The selection of the parameters for calibration is mainly based on the results of the sensitivity analysis. Some parameters responsible for X_H and X_A, such as saturation constant, decay coefficients, and some stoichiometric parameters listed in Table 6, are set to their default values as reported in the literature to reduce the number of parameters to be calibrated.

The calibrating parameter values are estimated by minimizing the sum of squares of the deviations between the measured data and the model predictions with the objective function given as below:

$$F(p) = \left(\sum_{i=1}^{n} (y_{\text{exp,i}} - y(p)_i)^2 \right)^{1/2} \tag{11}$$

where y_{exp} and $y(p)$ are vectors of n measured values and model predictions at times t_i (i from 1 to n), and p is the vector of the model parameters. The standard deviation in parameter determination is required to be $<50\%$ to ensure the validity of the values of the obtained parameters.

The model was calibrated according to a logical step-wise procedure (sludge production, nitrification, and denitrification) at two levels. The calibration at each level is not independent, because the processes incorporated in the model are coupled together. Consequently, several iterations with loops to the earlier stages are needed to complete the entire calibration procedure.

The model is calibrated at two levels with the characterization of the input wastewater and biomass: long-term simulation of the full-scale SBR performance and simulation of the batch tests. Initially, a series of dynamic simulations are performed to obtain the preliminary parameters that are related to the model outputs. The calibration approach at this level is to fit the model simulation results on the measured components, such as effluent COD and NH_4^+-N concentrations, and MLVSS data, which were measured in 60-day operation (March 4, 2007–January 2, 2007), by changing the calibrated parameters. The profiles of the model predictions and experimental observations for COD, NH_4^+-N, and MLVSS data are shown in Figures 4A–C, respectively. The calibrated model at this level is able to adequately simulate the variations of the effluent COD and NH_4^+-N concentrations as well as MLVSS data. Then, simulation is performed with the calibrated model to describe the batch experimental results. It is evaluated if the calibrated set of parameters at first step remained unchanged when the batch experimental results are described. However, the predictions for the OUR and N-dynamics are not satisfactory. Thus, the model has to be calibrated further.

The kinetic parameters concerning the nitrification and oxygen consumption processes are further estimated based on the batch test results. The values of the parameters adjusted after the calibration at two levels, along with the original set of parameters,[10,29] are listed in Table 6, whereas the batch simulation results are shown in Figure 5. The maximum difference between the measured and calculated values

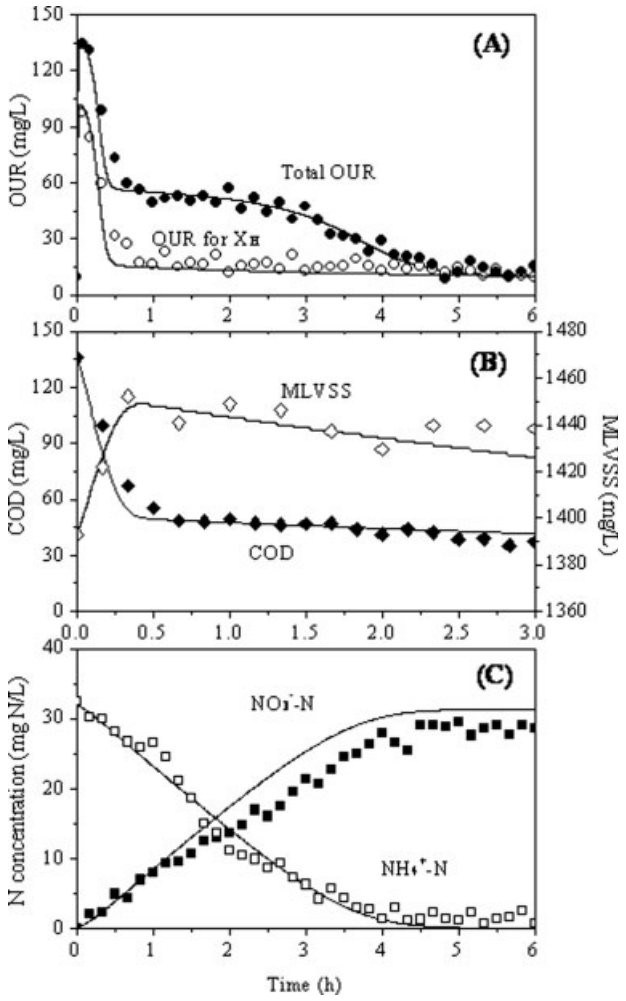

Figure 5. Measured and predicted results of the batch tests.

(A) Total OUR and OUR for X_H; (B) COD and MLVSS concentrations; and (C) N dynamics.

is 18 and 72% of the results have a difference of less than 5%, indicating that the model predictions match the batch test data. The values of the obtained parameters do not differ significantly from the average values obtained from a dynamic simulation during the long-term calibration period. The calibrated stoichiometric and kinetic parameter values in this study are generally comparable with those reported in the literature. [11,12,19,25,29–32]

Model evaluation with the long-term WWTP operating data

The experimental data, which are not previously used for model calibration, are used for model evaluation. The operating data of the WWTP during the period from March 5, 2007, to May 5, 2007, are used for model evaluation. The selected simulation results are illustrated in Figure 6 along with the calibrated parameters. The predicted effluent COD levels match the measured ones. Moreover, the model is capable of accurately simulating the short-term effects resulting from the variation of influent COD loading, in which high simulated peaks of COD are observed at the high influent COD levels (Figure 6A). A good prediction is also observed with respect to the effluent NH_4^+-N concentration and its disturbance (Figure 6B). The average difference between the simulations and measurements is <1.25 mg N L^{-1}. However, the difference between the simulated and measured MLVSS concentrations is about 20%. Even though such a value appears to be high, the model is able to reasonably predict the MLVSS changing trends (Figure 6C).

Model evaluation with the batch test data

Oxygen Consumption Batch Tests. The oxygen consumption tests show a good agreement between the predicted and observed data (Figure 7A). Simultaneous carbon oxidation and nitrification take place in this oxygen consumption test. The OUR peak in the initial several minutes is assumed to be attributed to the oxidation of S_S (dash line in Figure 7A). In this case, nitrification and oxidation of substrate released by hydrolysis occur (dash line in Figure 7A). This transition phenomenon for oxygen consumption curve can be simulated well with our model.

Nitrification Batch Tests. Nitrification in the batch tests is well predicted by the model (Figure 7B). In nitrification, the NH_4^+-N concentration decreases rapidly with time, suggesting utilization by the nitrifiers as an energy and nitrogen source. The nitrate concentration as the end product increases with time. The difference between the simulated and measured NH_4^+-N concentrations is $<15\%$, suggesting a good model prediction for ammonia utilization. The observed nitrate formation is approximately 20% higher than

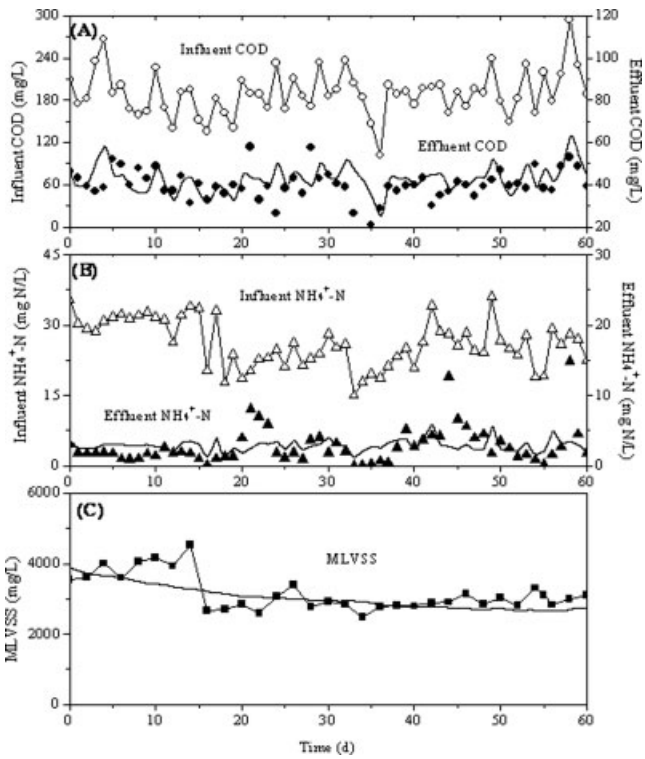

Figure 6. Measured and predicted results of the WWTP (May 5, 2007–March 5, 2007).

(A) COD level; (B) NH_4^+-N level; and (C) MLVSS concentration.

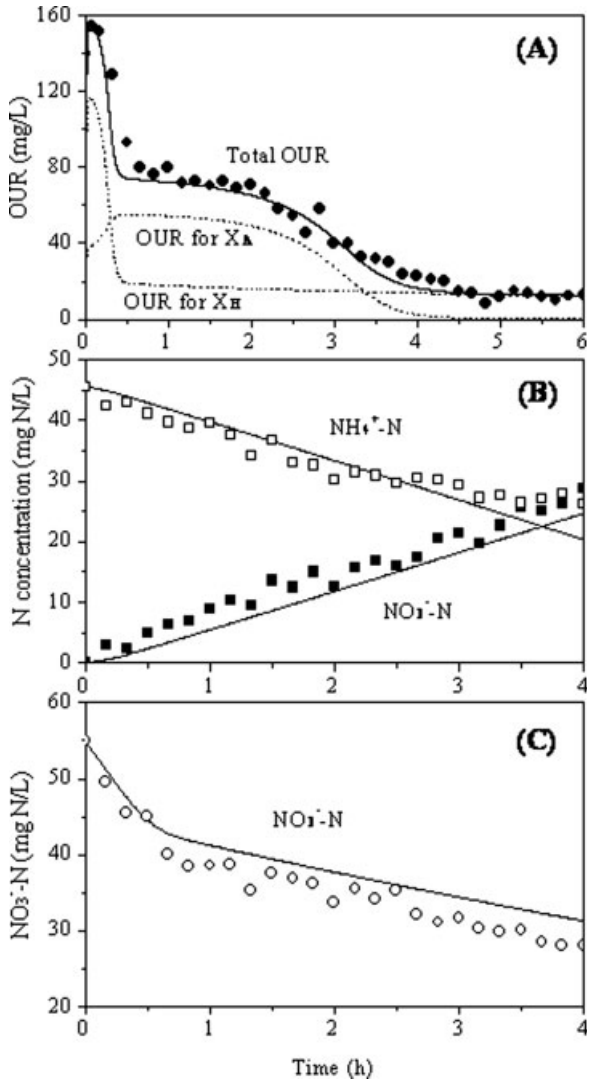

Figure 7. Model evaluation using the results from: (A) oxygen consumption batch tests; (B) nitrification batch tests, and (C) denitrification batch tests.

the predicted, but its changing trend could be predicted by the model.

Denitrification Batch Tests. The simulated and measured nitrate consumptions in the denitrification tests are shown in Figure 7C, in which two linear phases (slopes) of nitrate reduction rate are observed. The first slope is related to the denitrification on the influent S_S. This is followed by a lower denitrification rate resulting from the anoxic utilization of the delayed S_S from hydrolysis of X_S. Compared with the simulations, relatively rapid nitrate consumption is observed. However, the nitrate reduction in the two phases can be simulated well by the model.

Model simulation

Because of the enforcement of new national legislation for water quality control, the Zhuzhuanjing WWTP will be upgraded soon to meet the discharge standard requirements. To assess whether the existing capacity of this plant is sufficient for biological nitrogen removal, the verified model is used to explore the optimized operating strategies for nitrogen removal in this full-scale SBR plant. With the results from the calibration and evaluation of the present process in Zhuzhuanjing WWTP, the values of the toichiometric and kinetic parameters shown in Table 6 were adopted for model simulation. The simulation results show that high-quality effluent would be obtained if a 60-min anoxic phase was added into the running cycle of the SBR for denitrification and the reaction phase for COD removal and nitrification (Figure 8). The new operating strategy should be 45 min of influent filling, 60 min of anoxic denitrification, 150 min of aerobic react, 60 min of settling, and 45 min of effluent withdrawal. The total treatment capacity is not reduced (180 min influent filling per day). However, the operating costs associated with energy consumption can be reduced because of the decreased aerobic reaction time per day, but a high nitrogen removal could be achieved. These results further demonstrate that model simulation is able to provide a foundation for design and operation of biological WWTPs.

Conclusions

In this work, efforts were made to simulate the performance of a full-scale SBR plant for municipal wastewater treatment.

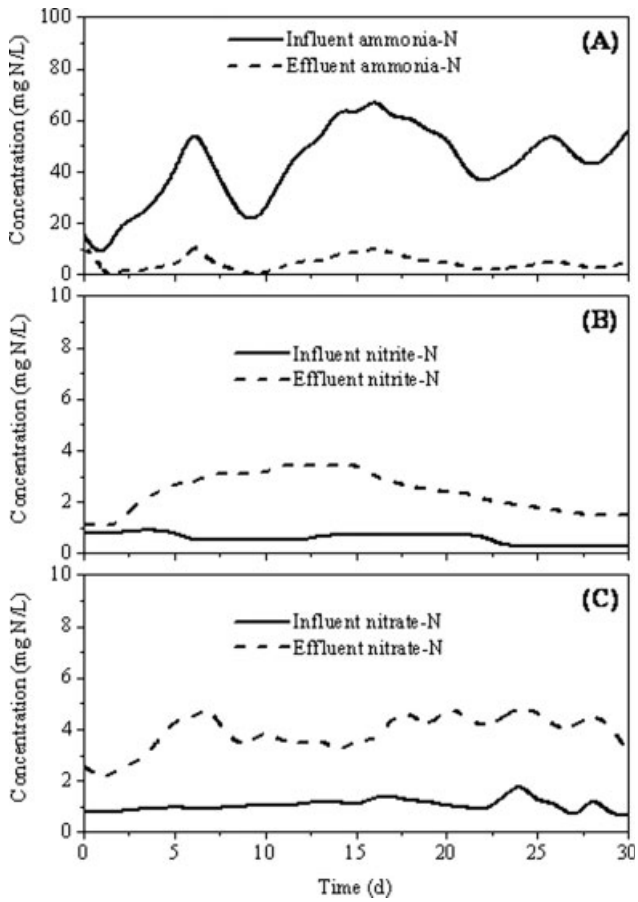

Figure 8. Model predictions for the full-scale SBR performance: (A) ammonia-N, (B) nitrite-N, and (C) nitrate-N.

After incorporating all the relevant processes and characterizing the municipal wastewater and activated sludge with batch tests, the modified ASM3 is found to be capable of simulating and predicting the 60-day performance of a full-scale SBR WWTP in terms of COD, NH_4^+-N, and MLVSS in the SBR system and the batch experimental data under different conditions. The sensitivity analysis suggests that the model parameters involved in the storage process, the heterotrophic endogenous decay, and growth have a great influence on the model outputs. The model is successfully calibrated and validated at two levels with the characterization of the input wastewater and biomass. Moreover, the model is able to accurately simulate the short-term effects resulting from the variation of influent COD loading. The modeling work in this article is useful for operation and optimization of full-scale SBR plants.

Acknowledgments

The authors thank the Natural Science Foundation of China (20577048, 50625825, and 50738006) the National Key Project for Water Pollution Control (2008ZX07103-001 and 2008ZX07316-003), and the Anhui R&D Key Project (07010301022 and 08010302109) for the partial support of this study.

Literature Cited

1. Irvine RL, Ketchum LH. Sequencing batch reactors for biological wastewater treatment. *Crit Rev Environ Control*. 1989;18:255–294.
2. Furumai H, Kazmi AA, Furuya Y, Sasaki K. Effect of sludge retention time (SRT) on nutrient removal in sequencing batch reactors. *J Environ Sci Health*. 1999;34:317–328.
3. de Kreuk MK, Heijnen JJ, van Loosdrecht MCM. Simultaneous COD, nitrogen, and phosphate removal by aerobic granular sludge. *Biotechnol Bioeng*. 2005;90:761–769.
4. Otawa K, Asano R, Ohba Y, Sasaki T, Kawamura E, Koyama F, Nakamura S, Nakai Y. Molecular analysis of ammonia-oxidizing bacteria community in intermittent aeration sequencing batch reactors used for animal wastewater treatment. *Environ Microbiol*. 2006;8:1985–1996.
5. Timur H, Ozturk I. Anaerobic sequencing batch reactor treatment of landfill leachat. *Water Res*. 1999;33:3225–3230.
6. Segar RL, Dwys SL, Speitel GE. Sustained trichloroethylene cometabolism by phenol-degrading bacteria in sequencing batch reactors. *Water Environ Res*. 1995;67:764–774.
7. Kortekaas S, Vidal G, He YL, Lettinga G, Field JA. Anaerobic-aerobic treatment of toxic pulping black liquor with upfront effluent recirculation. *J Ferment Bioeng*. 1998;86:97–110.
8. Irvine RL, Busch AW. Sequencing batch biological reactor—an overview. *J Water Pollut Control Fed*. 1979;51:235–243.
9. Gernaey KV, van Loosdrecht MCM, Henze M, Lind M, Jørgensen SB. Activated sludge wastewater treatment plant modelling and simulation: state of the art. *Environ Model Software*. 2004;19: 763–783.
10. Henze M, Gujer W, Mino T, van Loosdrecht MCM. *Activated Sludge Models ASM1, ASM2, ASM2d, and ASM3. IWA Scientific and Technical Report No. 9*. London, UK: IWA Publishing, 2000.
11. Henze M, Grady CPL Jr, Gujer W, Marais GVR, Matsuo T. *Activated Sludge Model No. 1. Scientific and Technical Report No. 1*. London: IAWPRC, 1987.
12. Gujer W, Henze M, Mino T, van Loosdrecht MCM. Activated sludge model no. 3. *Water Sci Technol*. 1999;39:183–193.
13. Reichert P. *Aquasim 2.0-User Manual, Computer Program for the Identification and Simulation of Aquatic Systems*. Dübendorf, Switzerland: EAWAG (ISBN 3 906484 16 5), 1998.
14. Siegrist H, Vogt D, Garcia-Heras JL, Gujer W. Mathematical model for meso- and thermophilic anaerobic sewage sludge digestion. *Environ Sci Technol*. 2002;36:1113–1123.
15. Spanjers H, Vanrolleghem P. Respirometry as a tool for rapid characterization of wastewater and activated sludge. *Water Sci Technol*. 1995;31:105–114.
16. Mathieu S, Etienne P. Estimation of wastewater biodegradable COD fractions by combining respirometric experiments in various So/Xo ratios. *Water Res*. 2000;34:1233–1246.
17. Roeleveld PJ, Van Loosdrecht MCM. Experience with guidelines for wastewater characterisation in The Netherlands. *Water Sci Technol*. 2002;45:77–87.
18. Grady CPL Jr, Daigger GT, Lim HC. *Biological Wastewater Treatment. Revised and Expanded*, 2nd ed. New York: Marcel Dekker, 1999.
19. Makinia J, Rosenwinkel KH, Spering V. Long-term simulation of the activated sludge process at the Hanover-Gummerwald pilot WWTP. *Water Res*. 2005;39:1489–1502.
20. Henze M. Characterization of wastewater for modelling of activated sludge processes. *Water Sci Technol*. 1992;25:1–15.
21. APHA. *Standard Methods for the Examination of Water and Wastewater*. 19th ed. Washington, DC: American Public Health Association, 1995.
22. Ni BJ, Yu HQ. Storage and growth of denitrifiers in aerobic granules. I. Model development. *Biotechnol Bioeng*. 2008;99:314–323.
23. Meijer SCF, van Loosdrecht MCM, Heijnen JJ. Modelling the start-up of a full-scale biological phosphorous and nitrogen removing WWTP. *Water Res*. 2002;36:4667–4682.
24. Sahlstedt KE, Aurola AM, Fred T. Practical modelling of a large activated sludge DN-process with ASM3. *Proceedings of the Ninth IWA Specialized Conference on Design, Operation and Economics of Large Wastewater Treatment Plants*,Czech Republic, Praha, September 1–4, 2003:141–148.
25. Koch G, Kuhni M, Gujer W, Siegrist H. Calibration and validation of activated sludge model no. 3 for Swiss municipal wastewater. *Water Res*. 2000;34:3580–3590.
26. Wichern M, Lubken M, Blomer R, Rosenwinkel KH. Efficiency of the activated sludge model no. 3 for German wastewater on six different WWTPs. *Water Sci Technol*. 2003;47:211–218.
27. Shahalam AB, Elsamra R, Ayoub GM, Acra A. Parametric sensitivity of comprehensive model of aerobic fluidized-bed biofilm process. *J Environ Eng-ASCE*. 1996;122:1085–1093.
28. Abasaeed AE. Sensitivity analysisona sequencing batch reactor model. I. Effect of kinetic parameters. *J Chem Technol Biotechnol*. 1997;70:379–383.
29. Sin G, Guisasola A, de Pauw DJW, Baeza JA, Carrera J, Vanrolleghem PA. A new approach for modelling simultaneous storage and growth processes for activated sludge systems under aerobic conditions. *Biotechnol Bioeng*. 2005;92:600–613.
30. Brdjanovic D, van Loosdrecht MCM, Versteeg P, Hooijmans CM, Alaerts GJ, Heijnen JJ. Modeling COD, N and P removal in a full scale WWTP Haarlem Waarderpolder. *Water Res*. 2000;34:846–858.
31. Rieger L, Koch G, Kuhni M, Gujer W, Siegrist H. The EAWAG bioP-module for activated sludge model no. 3. *Water Res*. 2001;35:3887–3903.
32. Moussa MS, Hooijmans CM, Lubberding HJ, Gijzen HJ, van Loosdrecht MCM. Modelling nitrification, heterotrophic growth and predation in activated sludge. *Water Res*. 2005;39:5080–5098.

Manuscript received July 6, 2008, and revision received Dec. 24, 2008.